J. Fluid Mech. (1975), *vol.* 70, *part* 3, *pp.* 463–479
Printed in Great Britain

Intensity, scale and convection of turbulent density fluctuations

By M. R. DAVIS

School of Mechanical and Industrial Engineering, University of New South Wales, Kensington, Australia 2033

(Received 2 September 1974)

This paper extends the quantitative schlieren technique to the separate determination of the local scales and intensity of turbulent density fluctuations. Measurements in an unheated supersonic jet are also extended to positions substantially further away from the jet than those reported hitherto, and show that high levels close to the nozzle reduce to levels comparable to subsonic velocity fluctuations beyond 18 diameters from the nozzle exit. Trends for the integral scales are similar to those based on subsonic jet velocity fluctuations. Separated-beam measurements show reflexion of disturbances on the jet centre-line just beyond the potential core. Spectra show a more peaked form close to the jet, and exhibit a rapid decrease in level with wavenumber.

1. Introduction

The use of a single-beam schlieren optical system to make quantitative measurements of density fluctuations has been described by Davis (1971, 1972). The distribution of the product of the intensity of density-gradient fluctuations and their integral scale across the flow was determined. A double-beam schlieren system with perpendicular beams was used by Wilson & Damkevala (1970), who related the cross-beam covariance to the density fluctuations at the intersection point under the assumption of local isotropy. The interpretation of both sets of measurements relied upon the detection beam being small in comparison with the flow integral scale perpendicular to the beam. Also, it required that the flow was approximately homogeneous over the region of significant correlation close to the detection point. The use of a double beam required the schlieren to be adjusted to sense the component of the density gradient perpendicular to both beams. All the measurements were made in the initial shear layer of the flow at $x/D = 1{\cdot}5$, $3{\cdot}0$ or $6{\cdot}0$, where x denotes distance from the exit plane and D the nozzle diameter at the exit plane. The distributions showed maxima in the shear layer which scaled with the density difference across the jet in the case of unheated flows. It appeared that the mixing of the cold jet with warmer surroundings was a determining factor in the intensity of fluctuation observed. Davis (1972) reported results for the product of the scale and intensity where this was eliminated by preheating the jet to a static temperature equal to that of the surroundings.

In the work to be described here, simultaneous single- and double-beam data were recorded and the results combined to determine distributions of both the fluctuation intensity and integral scale. The direct determination of the integral scale provided a check on the validity of the assumptions made in using the method as well as giving new basic information relating to the turbulent density structure. In addition, separated-beam measurements were made to determine the extent to which fluctuations in density are propagated with the flow. The results of Wilson & Damkevala (1970) showed an almost constant convection velocity across the shear layer of a subsonic jet, whilst the present work explored the variation in convection velocity much further downstream. The case selected for the present study was that of an unheated supersonic jet, measurements being made over a much larger range of distances from the jet than those for the earlier experiments. The general characteristics of cold supersonic jets may be inferred from the work of Potter & Jones (1967) and of Lowson & Ollerhead (1968). The shadowgraph results of the latter workers revealed the rather lower rate of mixing of a supersonic jet, although no detailed turbulent structure measurements were reported.

2. Principle of the method

As described by Davis (1971), the single-beam photodetector signal can be related linearly to the deflexion of the pencil ray striking the small photodetector aperture by

$$\Theta'_\zeta(Y) = A \int (\partial\rho/\partial\xi)' \, d\zeta. \tag{1}$$

A is a constant involved in the refractive-index relation for the medium, Y is the distance of the beam from the flow axis of symmetry, Θ'_ζ is the fluctuation in beam deflexion which modulates the output, $\partial\rho/\partial\xi$ is the gas density gradient in the flow direction and the beam is along the ζ direction. If the function $f_a(r)$ denotes the product of the fluctuation intensity and integral scale l, i.e.

$$f_a(r) = \left(\overline{\frac{\partial(\rho/\rho_0)}{\partial(\xi/D)}}\right)'^2 \frac{l}{D}, \tag{2}$$

where r is the radial distance from the flow axis, it follows that

$$\overline{\Theta'^2_\zeta(Y)} = \frac{2A^2\rho_0^2}{D} \int_Y^\infty f_a(r) \frac{r\,dr}{(r^2-y^2)^{\frac{1}{2}}}. \tag{3}$$

The measured profile $\overline{\Theta'^2_\zeta(Y)}$ can thus be used to determine the radial function $f_a(r)$.

The cross-correlation of two perpendicular beams with deflexions Θ_η and Θ_ζ gives rise to the following relation:

$$\overline{\Theta'_\eta \Theta'_\zeta} = A^2 \iint \overline{\frac{\partial\rho(x,y,z+\zeta)}{\partial\xi} \frac{\partial\rho(x,y+\eta,z)}{\partial\xi}} \, d\eta \, d\zeta. \tag{4}$$

It is assumed that the integration is carried out over the region of significant correlation of unsteady density gradients around $(x, y, z+\zeta)$ and $(x, y+\eta, z)$. Re-arrangement of this equation leads to the following relation:

$$\overline{\Theta'_\eta \Theta'_\zeta} = A^2\rho_0^2 \left(\overline{\frac{\partial(\rho/\rho_0)}{\partial(\xi/D)}}\right)'^2 \frac{l_\eta}{D} \frac{l_\zeta}{D}, \tag{5}$$

where l_η and l_ζ are the integral scales along each beam. Wilson & Damkevala (1970) showed that this correlation between two intersecting beams could, under the assumption of local isotropy, be related to the local density fluctuation:

$$\overline{\Theta'_\eta \Theta'_\zeta} = \frac{A^2 \rho_0^2}{2\pi} \overline{\left(\frac{\rho}{\rho_0}\right)'^2}. \tag{6}$$

As mentioned, the purpose of the present work is to determine distributions of $\overline{\Theta'^2_\zeta(Y)}$ simultaneously with distributions of $\overline{\Theta'_\eta \Theta'_\zeta}$, the beam along the ζ direction being traversed with Y across the flow and the beam along the η direction held in a fixed position through the flow centre-line. Application of (3) and (6) then yields $f_a(r)$ and $\overline{(\rho/\rho_0)'^2}$ as functions of radial distance from the centre-line, whilst combination of (5) with (3) gives an expression for the integral scale in the plane normal to the flow direction ($l = l_\eta = l_\zeta$ is assumed here, as before),

$$\frac{l}{D} = \frac{\overline{\Theta'_\eta \Theta'_\zeta}}{A^2 \rho_0^2} \frac{1}{f_a(r)}. \tag{7}$$

The intensity of the local density-gradient fluctuation follows from (5) as

$$\overline{\left(\frac{\partial(\rho/\rho_0)}{\partial(\xi/D)}\right)'^2} = \frac{(f_a(r))^2 A^2 \rho_0^2}{\overline{\Theta'_\eta \Theta'_\zeta}}. \tag{8}$$

Hence the simultaneous solutions for $f_a(r)$ and $\overline{\Theta'_\eta \Theta'_\zeta}$ may be used to determine the radial distributions of the integral scale and density-gradient intensity through (7) and (8).

Wilson & Damkevala also showed that, when the flow could be assumed to be locally homogeneous, the correlation of two orthogonal beams separated by ξ,

$$\overline{\Theta'_\eta(x,z)\,\Theta'_\zeta(x+\xi,y)} = A^2 \iint \frac{\partial^2}{\partial \xi^2} \overline{[\rho(x,y,z)\,\rho(x+\xi,y+\eta,z+\xi)]}\,d\eta\,d\zeta, \tag{9}$$

could be transformed by a one-dimensional Fourier transform into an energy spectrum

$$E_s(k_x) = \frac{1}{8\pi^3 A^2} \int_{-\infty}^{\infty} \overline{\Theta'_\eta(x,z)\,\Theta'_\zeta(x+\xi,y)} \exp(-ik_x\xi)\,d\xi, \tag{10}$$

where k_x is the wavenumber in the x direction. The function $E_s(k_x)$ was shown to be k_x^2 times the streamwise component of the three-dimensional density fluctuation spectrum function, i.e. $k_x^2 E_3(k_x, 0, 0) = E_s(k_x)$, where

$$E_3(k_x, k_y, k_z) = (8\pi^3)^{-1} \iiint \overline{\rho(x,y,z)\,\rho(x+\xi,y+\eta,z+\zeta)} \times \exp[-i(k_x\xi + k_y\eta + k_z\zeta)]\,d\xi\,d\eta\,d\zeta. \tag{11}$$

The function $E_s(k_x)$ can be determined by making the assumption of a convecting structure with a unique convection velocity U_c such that $\xi = U_c\tau$, where τ denotes a time delay, following the hypothesis of Taylor. Thus we may write

$$E_s(k_x) = \frac{U_c}{8\pi^3 A^2} \int_{-\infty}^{\infty} \overline{\Theta'_\eta(x,z,t)\,\Theta'_\zeta(x,y,t+\tau)} \exp(-ik_x U_c \tau)\,d\tau. \tag{12}$$

The application of this result to experimentally measured time correlation functions in a supersonic jet flow is considered in § 4. As will be shown, reflexion of disturbances at certain separations ξ and in certain parts of the flow causes the space correlation $R(\xi, 0)$, where

$$R(\xi, \tau) = \overline{\Theta'_\eta(x, z, t)\,\Theta'_\xi(x+\zeta, y, t+\tau)}/\overline{\Theta'^2_\eta}\,\overline{\Theta'^2_\xi},$$

to depart from the form expected for a convecting structure, in which case it is preferable to approach the energy spectrum by means of a transformation of a time correlation as given by (12) together with the known value of the convection velocity.

3. Experimental determination of scale and intensity

The unheated jet used had a nozzle exit diameter of 3·0 cm and was designed to have a parallel exit flow of Mach number 1·7, with an internal nozzle contour to provide a shock-free expansion of the flow. Measurement of the frequency spectrum of noise radiated by the jet showed that the discrete tone generated by the shock structure formed at stagnation pressures below the design value was eliminated as the stagnation pressure upstream of the nozzle was increased to the design value. Schlieren photographs of the flow were found to provide a rather less sensitive check that the nozzle was operating correctly at its design pressure ratio. However, variations of the upstream stagnation pressure by $\pm 10\,\%$ did show the formation of expansion waves at the lip when the pressure was too high and the formation of oblique shocks when it was set too low. It was concluded that the nozzle was operating correctly at its design pressure ratio. Although there was evidence of weak Mach waves forming from the lip and inside the nozzle, these could be discerned in the photograph of the first reflexion only, before becoming obscured by the turbulent structure. As no measurements were made with x/D less than 3·0, it was not expected that these waves would influence the results.

The schlieren detection system comprised two Spectral Physics helium–neon lasers of 1 mW power mounted on traversing mechanisms such that the beams were orthogonal. The traversing mounting also incorporated two United Detector Technology integrated-circuit deflexion-sensitive photodiodes. These produced, through an associated amplifier, a voltage proportional to the position of the incident light beam. The calibration of the system was found, by traversing the detector, to be linear over a range of 1 cm movement approximately. This arrangement has the advantage that deflexions larger than the measuring beam diameter (0·7 mm approximately) can be measured. The calibration can be related to the angular deflexion of the beam by the flow if the distance (0·63 m in this case) between the flow and the detector is known. This corresponds to a maximum deflexion of $\pm 10^{-2}$ rad, which is quite adequate for the measurements to be reported. A slight error is introduced in relating the detector output to the beam deflexion in this system owing to the thickness of the flow, but this is relatively small (of the order of 2 % in this case).

Correlation and mean-square values were measured using a Hewlett Packard 3721A digital correlator, one beam being held at a fixed location whilst the other

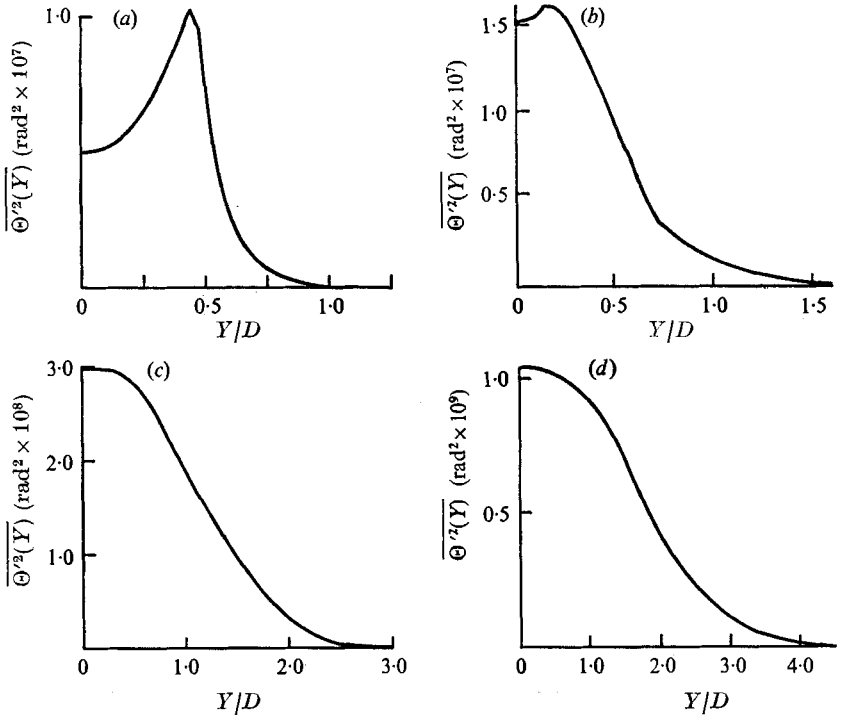

FIGURE 1. Mean-square angular deflexion of beam $\overline{\Theta_\zeta'^2(Y)}$. (*a*) $x/D = 3$, (*b*) $x/D = 9$, (*c*) $x/D = 18$, (*d*) $x/D = 25$.

was moved across the flow to intersect the fixed beam at different radial locations. Figure 1 shows a set of distributions of the function $\overline{\Theta_\zeta'^2(Y)}$ obtained from the moving beam at different axial locations, whilst figure 2 shows the corresponding set of covariance distributions $\overline{\Theta_\zeta'\Theta_\eta'(Y)}$. The curves have been based on approximately forty experimental points at equal intervals across the flow, the data being smoothed by differences. The data generally lay within 3 % of the curves shown. As discussed previously (Davis 1971), some smoothing is necessary if minor irregularities in the data are not to give rise to spurious peaks in the computed results when (3) is solved by numerical means. The distributions of covariance have also been interpreted in terms of the local density fluctuation intensity using (6), and sub-scales in figure 2 show the resulting values. It may be seen that the distributions show the expected change from an initial shear layer with a turbulent annulus to a distribution further downstream which shows only a small maximum off the jet centre-line.

The results of figures 1 and 2 transformed into distributions of the density-gradient intensity and integral scale are shown in figures 3 and 4. It may be seen that the distributions of the density-gradient intensity show generally similar development to that of the density fluctuations as would be expected. However, the distributions exhibit rather sharper peak values owing to the increase in integral scales away from the centre of the shear layer and jet axis. The distributions of the integral scale across the jet show in general a slightly lower value in

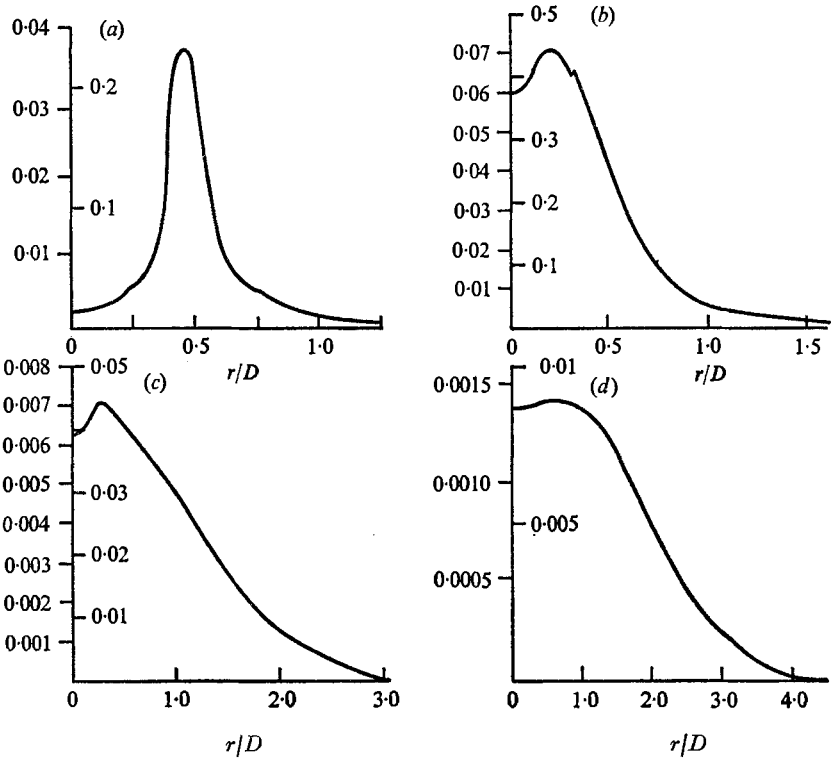

FIGURE 2. Radial distribution of two-beam covariance and density fluctuations. (a) $x/D = 3$, (b) $x/D = 9$, (c) $x/D = 18$, (d) $x/D = 25$. Ordinate scales: left-hand, $\overline{\rho'/\rho_0)^2}$; right-hand,

$$\frac{4\pi^2}{D^2}\overline{\left(\frac{\partial(\rho'/\rho_0)}{\partial(x/D)}\right)^2} l_\eta l_\zeta.$$

the centre of the shear layer than at the edges of the shear layer or at the outer edge of the flow further downstream. The profiles have been terminated outside regions of significant density fluctuations, as the application of (7) then gave rise to rather irregular results (as both numerator and denominator were small) and was subject to greater error. However, as figure 4 shows, where the density fluctuations were significant in relation to the maximum at any particular cross-section, relatively consistent results were obtained for the integral scales. It may be seen that at $x/D = 3{\cdot}0$ the integral scale is 0·15 times the jet diameter at the centre of the shear layer. This increases as would be expected at positions further downstream. The tendency for slightly higher values at the jet centre-line becomes less apparent further from the jet exit plane. Figure 5 shows that, whilst the initial increase of the integral scale is quite rapid, for distances beyond $x/D = 12$ a much slower rate of increase is observed. This result is in good agreement with the values for integral scales of axial-component velocity fluctuations in subsonic flow reported by Davies, Fisher & Barratt (1963) in the initial region of a jet, and also with the values reported by Wygnanski & Fielder (1969) further downstream in the self-preserving region of a subsonic jet. The present results

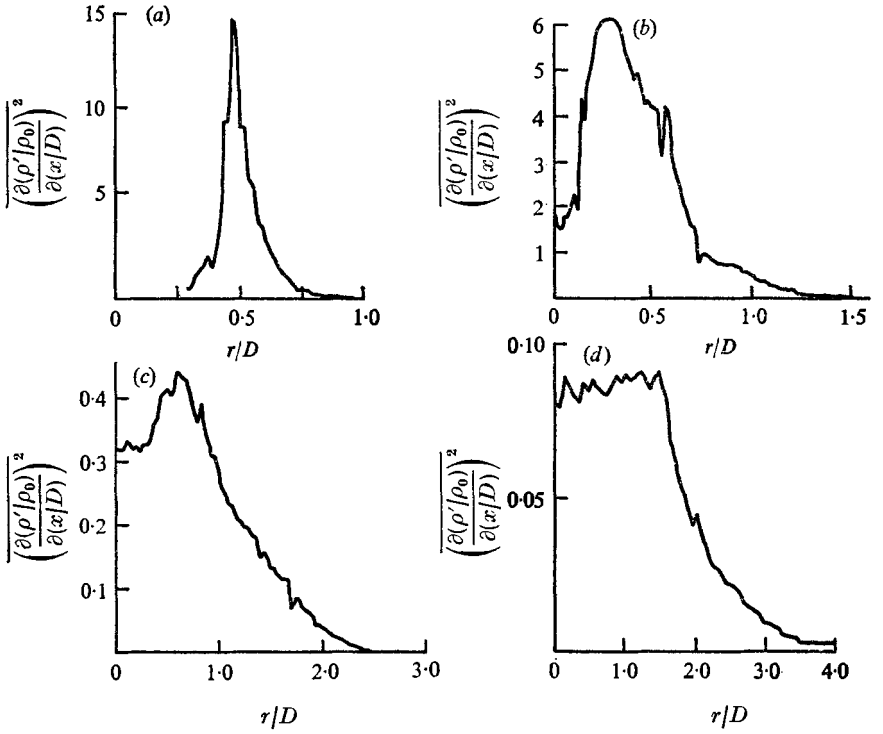

FIGURE 3. Radial distribution of fluctuating density gradient.
(*a*) $x/D = 3$, (*b*) $x/D = 9$, (*c*) $x/D = 18$, (*d*) $x/D = 25$.

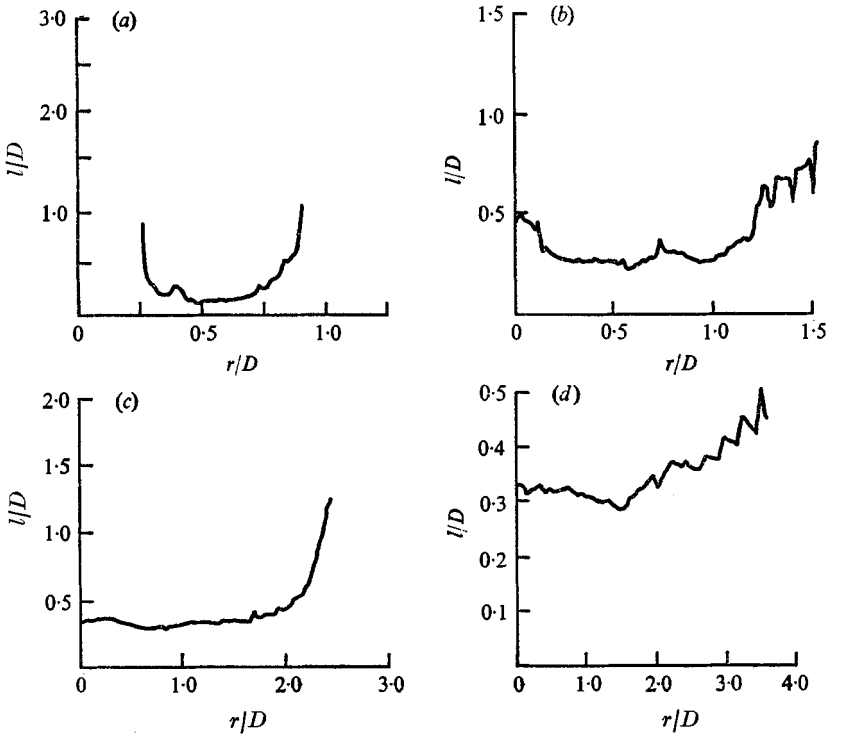

FIGURE 4. Radial distribution of integral scale *l*. (*a*) $x/D = 3$, (*b*) $x/D = 9$, (*c*) $x/D = 18$, (*d*) $x/D = 25$.

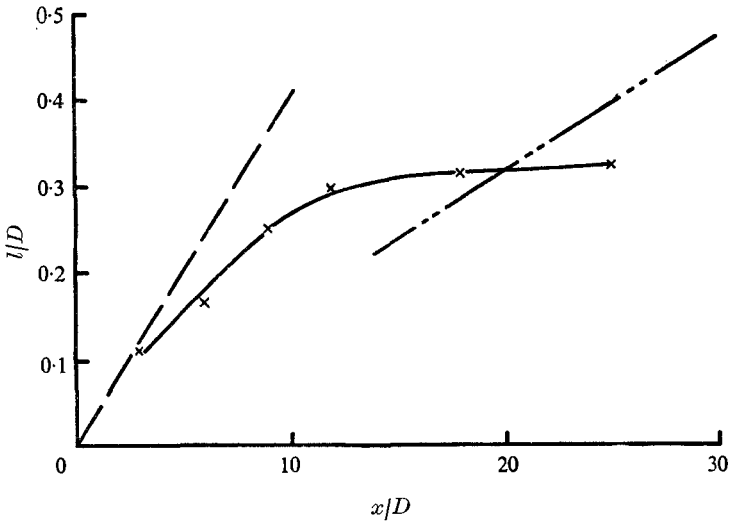

FIGURE 5. Axial distribution of integral scale. — —, Davies *et al.* (1963), $M_j = 0{\cdot}45$; — · · —, Wygnanski & Fielder (1969), $M_j = 0{\cdot}145$; — × —, present data, $M_j = 1{\cdot}7$.

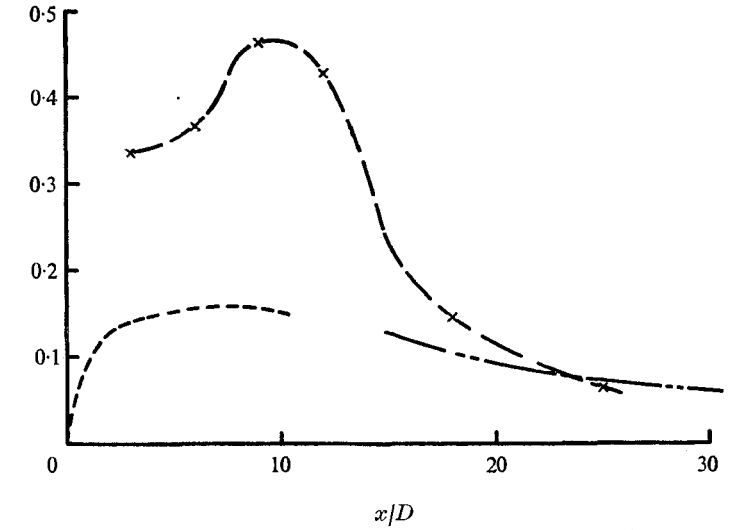

FIGURE 6. Axial distribution of maximum intensity. – – –, $(\overline{u'^2})^{\frac{1}{2}}/U_j$, Davies *et al.* (1963), $M_j = 0{\cdot}45$; — · · —, $(\overline{u'^2})^{\frac{1}{2}}/U_j$, Wygnanski & Fielder (1969), $M_j = 0{\cdot}145$; ——, $(\overline{\rho'^2})^{\frac{1}{2}}/(\rho_j - \rho_0)$, present data, $M_j = 1{\cdot}7$.

do however suggest a rather lower rate of increase of the integral scale for $x/D > 12$. The integral scale over the whole flow area studied exceeded the beam diameter by at least a factor of five. It appears therefore that the finite sizes of the detection beams have not influenced the interpretation of the measurements.

The variation of the maximum intensity at any cross-section with distance from the exit plane of the nozzle is shown in figure 6, normalized using the difference in density between the jet and its surroundings. It may be seen that high

relative intensities were observed close to the jet, reaching a maximum of 0·5 at $x/D \simeq 10$, whilst there is a rapid decrease in intensity beyond this position. Comparison of the results with normalized axial velocity fluctuation data for subsonic flows (figure 6) shows that beyond $x/D = 18$ similar relative intensities were measured. Whilst the diffusion of the jet in terms of its momentum and heat content might not be expected to be exactly similar (see, for example, Tyldesley (1969), where it appears that the turbulent diffusivity for heat exceeds that for momentum), it appears that the mixing intensities approach similar levels only at the positions investigated further away from the nozzle exit. Close to the jet, where much higher intensities were recorded, it appears therefore that turbulent compression of the flow is a contributing factor to the observed fluctuation. The magnitudes of the levels recorded at $x/D = 3$, 6 and 9 indicate that, unless the amplitude distribution of the density fluctuations departs strongly from Gaussian form, the local density varies outside the range between the densities of the jet and the surrounding air. Such perturbations would imply that turbulent compression effects are significant in the observed variations. Comparison of the values of $f_a(r)$ obtained previously (Davis 1971, 1972) close to the jet exit with those in figure 3 (*a*) shows that the present results are approximately twice the values extrapolated from subsonic unheated jet data. Estimation of the contribution due to turbulent compressive stress from data for the larger heated supersonic jets obtained previously suggests that this would only partially account for (approximately 20 % at $x/D = 3$) the high values obtained in the present work. This conclusion is supported by the relatively low core fluctuations detected here; in the heated supersonic jet the core fluctuations were more comparable to those in the shear layer. It is concluded that, whilst the present data at $x/D = 3$, 9 and 12 contain substantial contributions due to turbulent compressive stress, a major contributing factor is the effect of mixing. However, as the effects would interact in the fluctuating momentum flux of the flow it appears unrealistic to expect that they would be accumulative as if statistically independent. The rather high values obtained here appear to indicate some interaction. Whilst it might be possible to attribute the high levels observed to unsteady movements of the shear layer as a whole (where it is well defined), the observation of strong fluctuations over the whole region $3 < x/D < 12$ would suggest that turbulent compression is a contributing factor. Indeed, the intensities observed at $x/D = 9$ and 12 are somewhat higher than those at $x/D = 3$ and 6 and suggest that gross movement of the whole shear layer (which would not be well defined at the former positions) does not explain the observations. Further the possibility of a shock wave influencing the measurements substantially does not appear likely for several reasons. First, the measurements were not found to be extremely sensitive to the position along the jet, as might be the case if local shocks were influencing the results. Second, the integral scale at the region of maximum intensity (figure 4) was not unduly large as might be expected if a shock wave were present. Third, the intensity increased somewhat between $x/D = 3$ and 12, whereas a shock effect would be expected to weaken as the jet diffused.

The transverse distribution of the fluctuating intensity also shows departures from the form of subsonic velocity fluctuation data. At $x/D = 6$ for example, the

maximum-intensity position is $r/D = 0{\cdot}46$, whereas the distribution of subsonic velocity fluctuations in the shear layer shows a maximum at r/D close to 0·5 (see Davies *et al.* 1963). This movement is due to the presence of turbulent compressive effects in the observed density fluctuations, as these would be more highly weighted towards the regions of higher local velocity towards the inner edge of the shear layer. Also, the overall spread of the distribution of intensity based on positions of half maximum intensity is much less, being equivalent to values of $\Delta r/D$ of 0·21 and 0·30 at $x/D = 3$ and 6 respectively, whereas the subsonic velocity fluctuation data gave corresponding values of $\Delta r/D = 0{\cdot}34$ and 0·68 at a Mach number of 0·45. This reflects the greater proportionate increase in density fluctuations with turbulent compression, although the results further downstream suggest that it may also be influenced by the slower decay of the jet velocity and correspondingly slower transverse diffusion. At $x/D = 18$ and 25, the density fluctuations reduce to half their centre-line values at $r/D = 0{\cdot}09$ and 0·10 respectively, whereas the subsonic velocity fluctuation results reduce to half the centre-line intensity at $r/D = 0{\cdot}15$ (see Wygnanski & Fiedler 1969). As turbulent compression appears to be less significant further from the jet exit, this smaller transverse spread of the region of fluctuations at large distances from the nozzle exit is almost certainly due primarily to the reduced transverse diffusion of the cold supersonic jet.

4. Separated-beam correlation measurements

Typical results for space and time separated correlations are shown in figure 7 for positions in the initial shear layer and on the centre-line immediately beyond the end of the potential core and far downstream. In all three cases it may be seen that the location of the maximum correlation clearly indicates a convection velocity for the flow. This is shown by the close fit to a straight line of the time location of the peak as a function of separation. The maximum velocities obtained on the centre-line (or in the shear layer for $x/D < 6$) are compared with other measurements of mean velocity in figure 8, the data shown for the $M = 1{\cdot}8$ nozzle having been obtained from stagnation-pressure data. It may be seen that the results indicate that both the mean and convection velocity for supersonic initial conditions decrease more slowly with distance from the nozzle exit. The results suggest that the displacement of the apparent origin of any ultimate self-preserving behaviour for the initially supersonic jet would be significantly greater than that observed in subsonic cases (see Wygnanski & Fiedler 1969). It also appears that the maximum convection velocity is rather smaller in relation to the local mean velocity than was the case for the subsonic flows.

The transverse distribution of convection velocity is shown in figure 9, the values obtained here being based on cross-correlations measured with a 3 cm beam separation. It may be seen that further away from the jet ($x/D > 12$) the results appear to collapse when normalized using the maximum velocity and distance from the jet. The transverse diffusion of momentum is clearly shown to be smaller than for a subsonic case, this being consistent with the slower decay of maximum velocity. Close to the jet this normalization of the data is not found

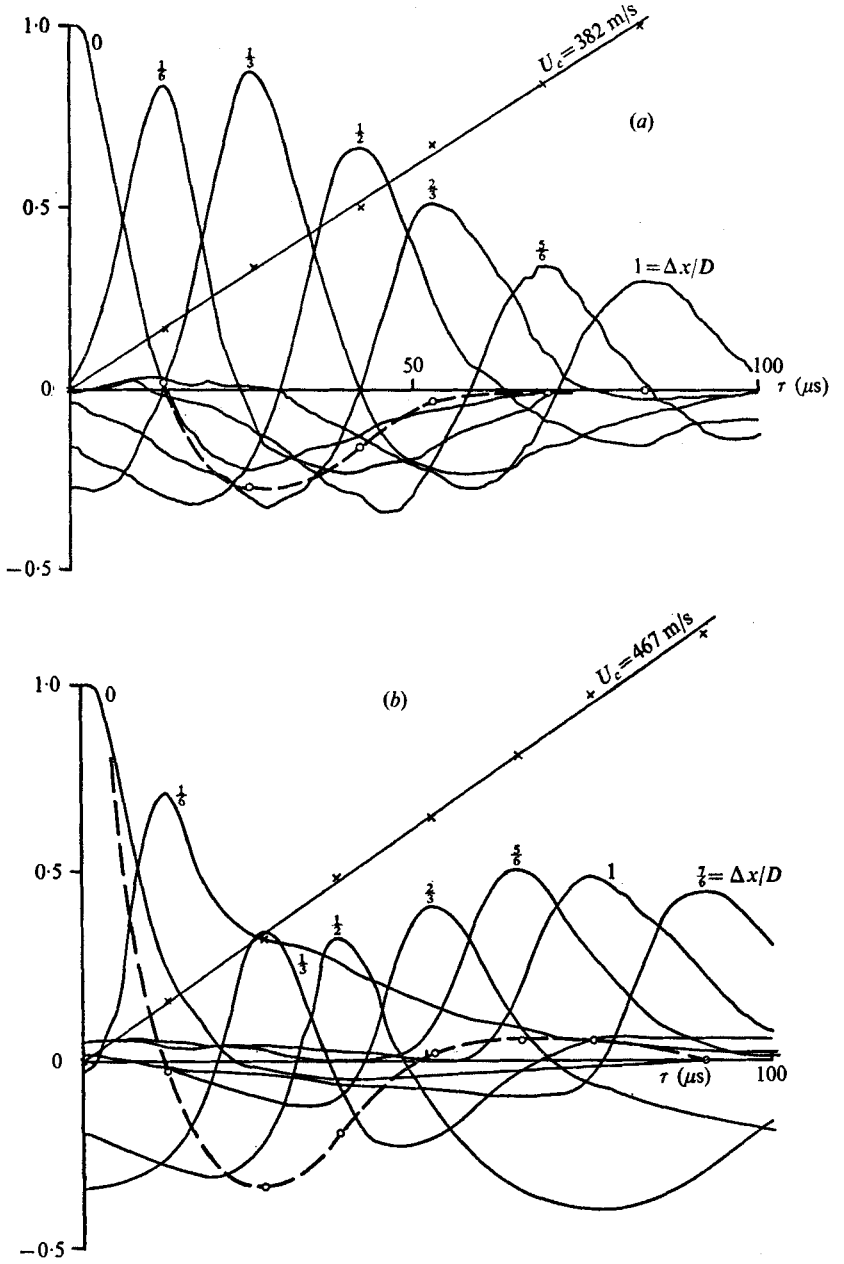

FIGURES 7 (*a*, *b*). For legend see next page.

to be appropriate, as is shown by the results at $x/D = 9$ in figure 9. It may be seen that the measured convection velocity appears to increase at the outer edges of the jet, where the local intensities are quite low. Similar increases were observed at $x/D = 3$ and 6, whilst a lower convection velocity was indicated for these latter cases at the inner edge of the shear layer. These results suggest that the fluctuations to either side of the initial shear layer are characterized by a velocity more

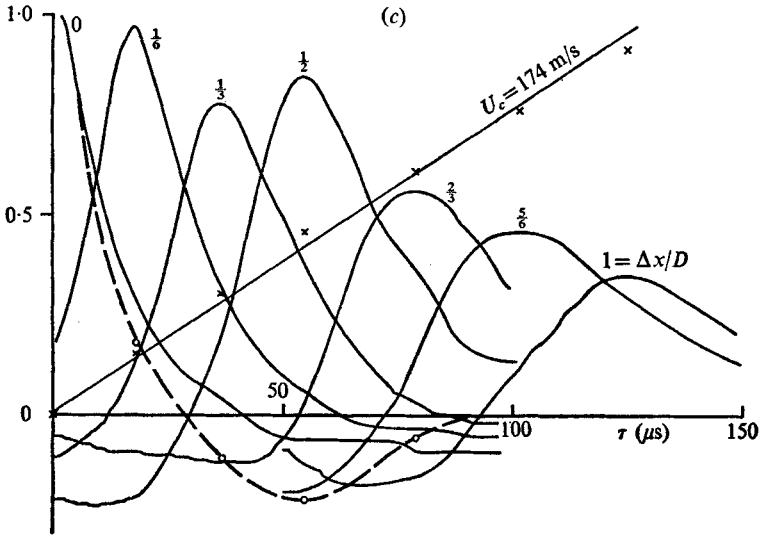

FIGURE 7. Space–time correlation functions. ——, $R_{\eta\zeta}(\Delta x/D, \tau)$; —×—, $\Delta x_m/D$ (line slope = U_c; U_j = 485 m/s); ---o---, $R_{\eta\zeta}(\Delta x/D, \Delta x/U_c)$. (*a*) $x/D = 3$, $r/D = 0{\cdot}5$; (*b*) $x/D = 9$, $r/D = 0$; (*c*) $x/D = 18$, $r/D = 0$.

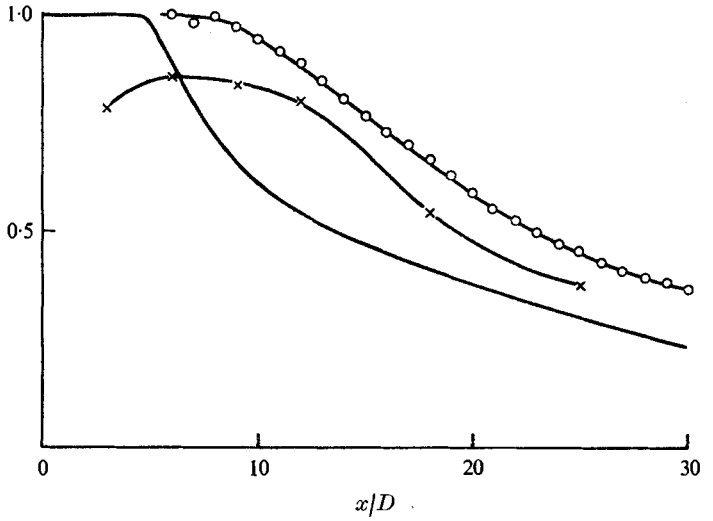

FIGURE 8. Axial distribution of centre-line velocity. ——, $\overline{U}/U_j$, Wygnanski & Fiedler (1969), $M_j = 0{\cdot}145$; —o—, $\overline{U}/U_j$, Pitot data, $M_j = 1{\cdot}8$; —×—, U_c/U_j, crossed schlieren data, $M_j = 1{\cdot}7$.

similar to that in the shear layer than the local velocity. This indicates that these disturbances are a result of disturbances produced within the region of maximum intensity. Similar effects were reported by Wilson & Damkevala (1970), who noted an unusually small variation in convection velocity close to the nozzle exit. It should be noted that in the present results the observations of velocities which depart from the form of a monotonic decrease with radius were made in regions where the local intensity was quite low.

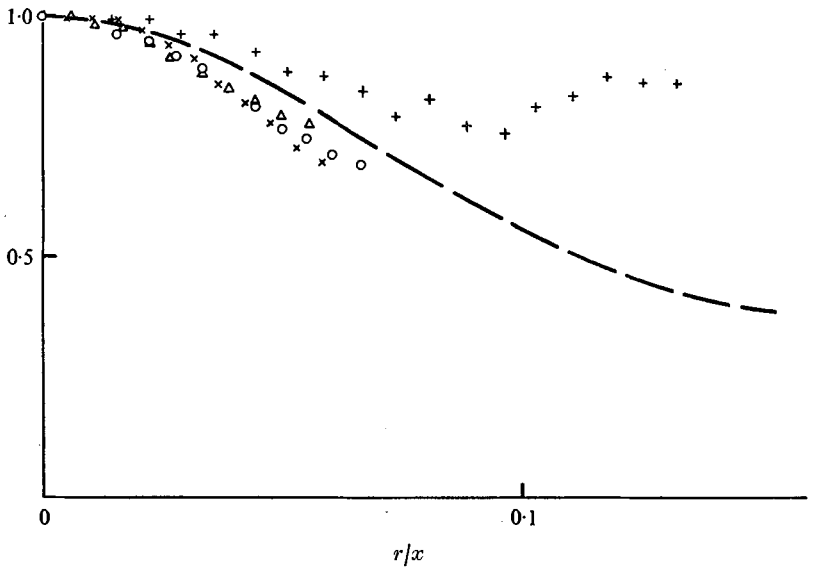

FIGURE 9. Transverse distribution of local mean velocity. $U_c/\bar{U}_m$, crossed schlieren data: ×, $x/D = 25$; ○, $x/D = 18$; △, $x/D = 12$; +, $x/D = 9$. – – –, $\bar{U}/\bar{U}_m$, Wygnanski & Fiedler (1969), $M_j = 0{\cdot}145$.

Whilst the cross-correlation results (figure 7) at $x/D = 3$ show a steady decay in the maximum correlation, at $x/D = 9$ there is evidence of a departure from this for moderate separations. The correlation $R(\Delta x/U_c)$ is also shown for comparison, and it may be seen that there is a strong departure from a form consistent with that of a convecting decaying structure. This effect was also observed at $x/D = 12$ on the centre-line, and to a lesser extent at $r/D = 0{\cdot}5$ at both positions. At the other positions where measurements were made ($x/D = 3$, 6, 18 and 25) the marked minimum in the maximum correlation at moderate separation was not observed. The results at $x/D = 9$ and 12 suggest that a negatively correlated component of rather longer time scale is superimposed on the convected peak. However, it does not appear to have significantly altered the estimation of convection velocity as the convected peak is relatively sharp. Transformation of the cross-correlation (obtained over a time-delay range $-200 < \tau < 300\,\mu$s in $1\,\mu$s intervals) into amplitude and phase co-spectra shows this more clearly (figure 10). At the separation where the effect is strongest the co-spectral density shows two distinct maxima, whilst the phase spectrum shows negative values over the lower range of frequencies. At the larger separation it may be seen that the lower frequency peak is no longer present. As it was found that for the larger separation the phase spectrum showed no negative values but a monotonic increase with frequency, the result for this case has been shown in terms of the equivalent phase velocity ($\Delta xw/\phi(w)$, where $\phi(w)$ is the phase spectrum). It may be seen that the phase velocity at the larger separation is relatively constant, although apparently increasing somewhat at higher frequency. This suggests that there is a return to characteristics suggesting a convecting structure at larger separations. Since the velocity measurements indicate this to be a region of supersonic mean velocity,

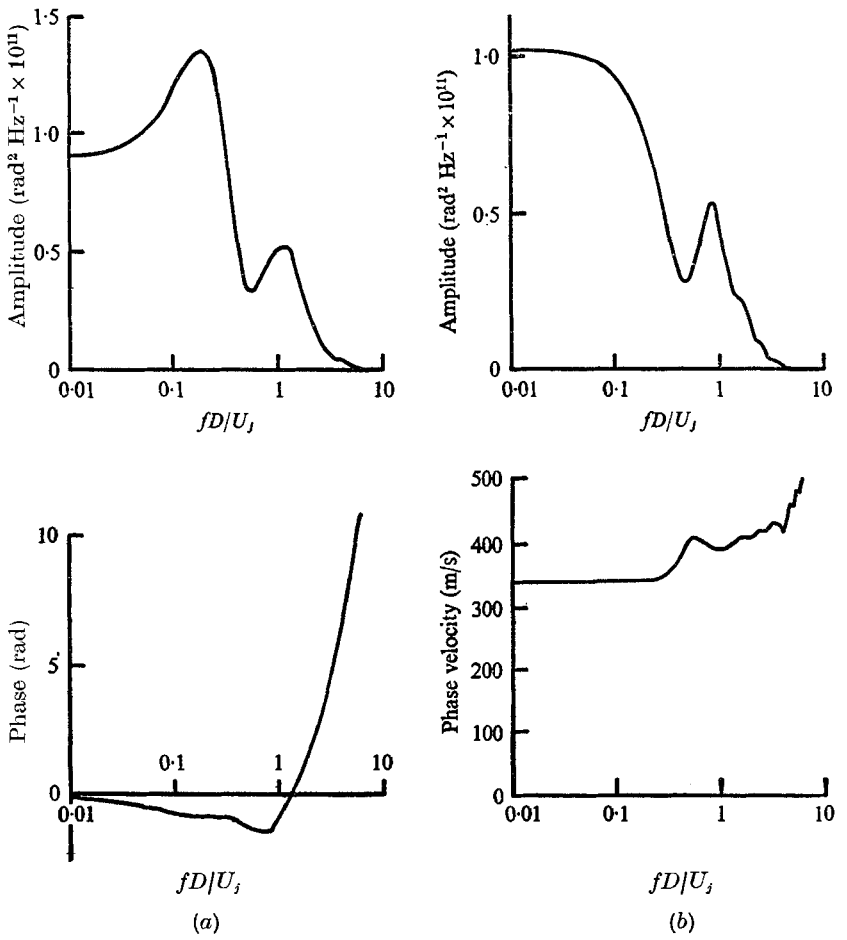

FIGURE 10. Co-spectra of dual beam deflexions, $x/D = 9$, $r/D = 0$. (*a*) $\Delta x/D = \frac{1}{3}$, (*b*) $\Delta x/D = 1$.

it appears that the negatively correlated component represents a reflexion of disturbances with a change of sign from the effective flow boundary in a symmetric manner causing reinforcement at the centre-line. The apparent absence of the effect at the larger separation suggests that the first reflexion only is significant. The restriction of the effect to positions in turbulent supersonic flow on the centre-line supports the hypothesis that it is caused by a reflexion mechanism. It would appear also that, if the effect were significant for small and zero beam separations, it would lead to increased integral scales in the flow. As these were not greatly increased at $x/D = 9$ and 12, it is concluded that the effect is only significant when correlation of two-point disturbances corresponds to a position where symmetric reflexion from the flow boundary gives a negatively correlated component which is not directly convected with the flow. This argument is supported by the weakening of the effect away from the jet axis. The results indicate that the density fluctuation field will contain components due to propagation of disturbances from neighbouring positions, although the convected mixing effects

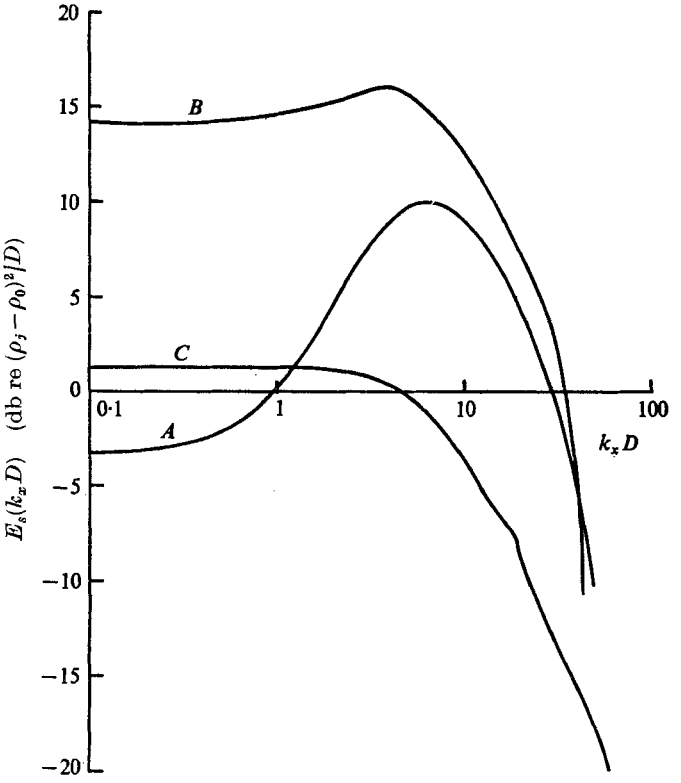

FIGURE 11. Energy spectra. *A*, $x/D = 3$, $r/D = 0{\cdot}5$; *B*, $x/D = 9$, $r/D = 0$; *C*, $x/D = 25$, $r/D = 0$.

tend generally to predominate. At $x/D = 18$ (figure 7 *c*) there is still evident some difference between $R(\Delta x/Uc)$ and $R(\tau)$, although not as great as that at $x/D = 9$. Closer agreement was observed at $x/D = 25$, indicating that the effect of negatively correlated reflected disturbances was becoming less significant as the flow velocity reduced, as would be expected. It may be seen from figure 7 that the effect at $x/D = 9$ is observed most strongly for a separation corresponding to $\Delta x \simeq 1{\cdot}25$ cm. At this position, only the central portion of the flow would be supersonic, and a short axial separation for positions showing negative correlation would be expected.

Where the two detection beams intersect with zero separation, transformation of the cross-correlation function may be used to determine the energy spectrum $E_s(k_x)$ or $E_3(k_x, 0, 0)$, provided that it is assumed that the structure convects at a characteristic velocity. From the foregoing discussion it appears that this will be a fair approximation provided that the cross-correlation is not strongly influenced by reflexion effects, which appear to be significant only at certain beam separations and positions in the flow. The result of transforming the symmetric correlation function at zero separation for three positions in the flow is shown in figure 11. As the highest frequency analysed in all cases corresponded to a period equal to ten time increments on the correlation diagram, and since this time also

corresponds to the time for the flow to convect across the total width of the detection beam, errors due to the transformation process and due to the finite spatial resolution of the detection beams should not be significant in the spectra shown. It may be seen that in the initial shear layer of the jet the energy spectrum $E_s(k_x)$ shows a strongly peaked form having a maximum at $k_x \simeq 6/D$. This indicates the scale of the strongest disturbances to be approximately the shear-layer thickness. Further downstream at $x/D = 9$ on the jet centre-line, the peak in the energy spectrum is much less pronounced although the overall level has increased, in particular at the lower wavenumbers. The peak is now located at $k_x = 4/D$, there being a movement towards lower wavenumbers as might be expected. At $x/D = 18$ the spectrum shows no peak at all and the overall level appears to have decreased fairly uniformly from that at $x/D = 9$. Whilst it is not possible to identify clearly any section of the spectra as having a characteristic decay form at high wavenumbers, it may be seen that there is a relatively sharp decrease with wavenumber to approximately $k_x = 30/D$, beyond which the negative slope increases still further. The spectra fall off approximately as the square of the wavenumber up to this value, suggesting that $E_3(k_x, 0, 0)$ would decrease as the fourth power of wavenumber. In general, the spectra appear to illustrate the change from fluctuations constrained to a certain maximum scale by the geometry of the shear layer to a form where such a constraint is not evident in the flow further downstream. Peaked frequency spectra were also observed for subsonic density fluctuations by Davis (1971) and for velocity fluctuations by Bradshaw, Ferriss & Johnson (1964), and it appears therefore that this effect is due to the confinement of the fluctuations within the shear layer.

5. Conclusions

The integral scales for the density fluctuations in an initially supersonic jet show general trends similar to those for velocity fluctuations in subsonic flows. The intensity of the density fluctuations was found to be relatively high close to the jet. Unless the amplitude probability distribution of the turbulent density fluctuations departed strongly from Gaussian, it would follow that the density excursion lay substantially outside the range extending from the density of the ambient air to that of the jet. The intensity returns to levels comparable with subsonic velocity fluctuations at $x/D = 18$. The high levels appear to be due to the combined effects of mixing, turbulent stress and reflexion of disturbances in the region of the jet just beyond the end of the potential core causing reinforcement close to the jet axis. Evidence for reflexion effects was found in cross-correlations with separated beams, although the measurements still gave a clear indication of disturbances convected with the flow. Reflexions appear to influence the results for certain separations of the detection points close to the jet axis at $x/D = 9$ and 12 in the present results, and would partially account for the unusually high fluctuation intensity observed at these positions. Measurements of the mean and convection velocity show the jet to diffuse relatively more slowly than a subsonic jet, as was also shown by Potter & Jones (1967) and others. Towards the region of the flow where density fluctuations were weaker but

adjacent to regions of strong fluctuation, measurements of local convection velocity gave values which did not reduce as expected at the edge of the flow and did not approach the jet velocity in the inner region of the shear layer. This suggests that in this portion of the flow local density fluctuations are caused by propagation of disturbances from the most strongly turbulent region and characterized by the velocity in that region. Further away from the nozzle where the maximum intensity was lower, the transverse distribution of convection velocity showed a more consistent decrease with distance from the centre-line. The mean velocity profiles appeared then to follow a simple scaling with distance from the nozzle. Spectra for density fluctuations showed a more strongly peaked form in the shear layer than at positions further away from the jet exit.

The author wishes to acknowledge the support of the United Kingdom Science Research Council through a grant to Professor P. O. A. L. Davies. The assistance of the staff of the Institute of Sound and Vibration, University of Southampton, and the helpful advice of Mr M. Harper-Bourne are also acknowledged.

REFERENCES

Bradshaw, P., Ferriss, D. H. & Johnson, R. F. 1964 Turbulence in the noise-producing region of a circular jet. *J. Fluid Mech.* **19**, 591–624.

Davies, P. O. A. L., Fisher, M. J. & Barratt, M. J. 1963 The characteristics of the turbulence in the mixing region of a round jet. *J. Fluid Mech.* **15**, 337–367.

Davis, M. R. 1971 Measurements in a subsonic turbulent jet using a quantitative schlieren technique. *J. Fluid Mech.* **46**, 631–656.

Davis, M. R. 1972 Quantitative schlieren measurements in a supersonic turbulent jet. *J. Fluid Mech.* **51**, 435–447.

Lowson, M. V. & Ollerhead, J. B. 1968 Visualization of noise from cold supersonic jets. *J. Acoust. Soc. Am.* **44**, 624–630.

Potter, R. C. & Jones, J. H. 1967 An experiment to locate the acoustic sources in a high speed jet exhaust stream. *J. Acoust. Soc. Am.* **42**, 1214.

Tyldesley, J. R. 1969 Transport phenomena in free turbulent flows. *Int. J. Heat Mass Transfer*, **12**, 489–496.

Wilson, L. N. & Damkevala, R. J. 1970 Statistical properties of turbulent density fluctuations. *J. Fluid Mech.* **43**, 291–303.

Wygnanski, I. & Fiedler, H. 1969 Some measurements in the self-preserving jet. *J. Fluid Mech.* **38**, 577–612.